QUADRUPOLAR TRANSVERSE IMPEDANCE OF SIMPLE MODELS OF KICKERS

B. Salvant, N. Mounet, C. Zannini EPFL, Lausanne/CERN, Geneva, Switzerland
E. Métral, G. Rumolo CERN, Geneva, Switzerland

Abstract

The SPS kickers are major contributors to the SPS transverse beam coupling impedance. The current "flat chamber" impedance model for a kicker is obtained by applying form factors to the theoretical impedance of an axisymmetric ferrite beam pipe. This model was believed to be acceptable for the vertical dipolar impedance, as two-wire measurements on SPS kickers revealed a satisfactory agreement. However, one-wire measurements on PS kickers suggested that this model underestimates the kickers' transverse quadrupolar (detuning) impedance. The longitudinal and transverse dipolar impedances of another kicker model that accounts for the metallic plates on each side of the ferrite were derived in the past by H. Tsutsui. The same formalism is used in this paper to derive the quadrupolar impedance. These formulae were then successfully benchmarked to electromagnetic (EM) simulations. Finally, simulating the interaction of an SPS bunch with the improved kickers' model results in a positive horizontal tune shift, which is very close to the tune shift measured with the SPS beam.

INTRODUCTION

The vertical dipolar impedance computed with the flat chamber model was successfully benchmarked to 2 wire impedance measurements up to 1 GHz for an SPS MKE kickers [1]. The dipolar vertical impedance in this frequency range is expected to be the most critical as far as SPS single bunch transverse stability is concerned. However, this flat chamber model obtained from Zotter/Métral theory [2] with Yokoya factors [3] can not explain the negative total horizontal impedance measured on a PS kicker with a single wire in a certain frequency range [4]. In fact, using Yokoya factors, the total horizontal impedance can only be positive or zero. As a consequence, E. Métral suspected that the actual quadrupolar horizontal impedance should be larger than the dipolar horizontal impedance in absolute value [5], and pointed at the fact that this flat chamber model does not take into account the vertical metallic plates on each side of the ferrite blocks. Earlier, in order to refine the cylindrical model for the kickers, H. Tsutsui had already derived a field matching theory to obtain the longitudinal [6] and transverse dipolar [7] impedance of a geometrical model with vertical metal electrode plates described in Fig. 1 for an ultrarelativistic beam. In these references, his theoretical dipolar impedance calculations were compared to *HFSS* simulations and subsequently to measurements of PS and SPS kickers in Refs. [4], [8] and [9]. It would be interesting to be able to use this impedance formalism to generate transverse wake functions that could be imported into *HEADTAIL*. In his paper [7], H. Tsutsui only derived the transverse dipolar impedances. In this paper, we derive the quadrupolar impedance from the source and EM fields obtained for the calculation of the longitudinal impedance in [6].

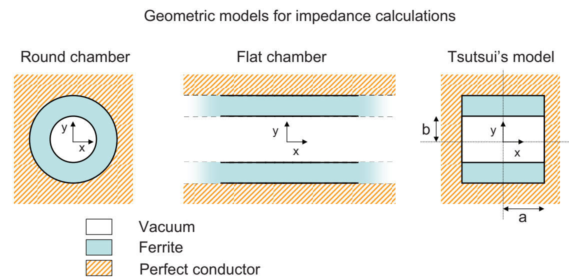

Figure 1: Geometric models for theoretical impedance calculations: cylindrical model (left), flat chamber model (center), model that accounts for perfect conducting plates on both sides of the ferrite plates (right).

IMPEDANCE DERIVATION

H. Tsutsui computed the fields in the vacuum region ($y < b$ and $x < a$) (Eq. (17) in Ref. [6]):

$$\begin{aligned}
E_z(x,y) &= \sum_n (A_n + B_n)\cos(k_{xn}x)\cosh(k_{xn}y)\,, \\
E_x(x,y) &= \sum_n \frac{jk}{k_{xn}} A_n \sin(k_{xn}x)\cosh(k_{xn}y)\,, \\
E_y(x,y) &= \sum_n \frac{jk}{k_{xn}} B_n \cos(k_{xn}x)\sinh(k_{xn}y)\,, \\
Z_0H_z(x,y) &= \sum_n (A_n + B_n)\sin(k_{xn}x)\sinh(k_{xn}y)\,, \\
Z_0H_x(x,y) &= j\sum_n \left(\frac{k_{xn}}{k}A_n + \left(\frac{k_{xn}}{k} - \frac{k}{k_{xn}}\right)B_n\right) \\
&\quad \times \cos(k_{xn}x)\sinh(k_{xn}y)\,, \\
Z_0H_y(x,y) &= j\sum_n \left(\left(\frac{k_{xn}}{k} + \frac{k}{k_{xn}}\right)A_n + \frac{k_{xn}}{k}B_n\right) \\
&\quad \times \sin(k_{xn}x)\cosh(k_{xn}y)\,,
\end{aligned} \tag{1}$$

with $k_{xn} = \frac{(2n+1)\pi}{2a}$, where $Z_0 = \mu_0 c$ is the vacuum impedance. The time and longitudinal dependences $\exp(j\omega(t - z/c))$ are omitted. Full derivations of EM fields in similar rectangular waveguide models loaded with dielectric slabs are given in Refs. [10] and [11].

Horizontal Quadrupolar Impedance

At coordinate $(x, y) = (\xi, 0)$, fields E_x and H_y in the vacuum region can be written

$$E_x(\xi, 0) = \sum_n \frac{jk}{k_{xn}} A_n \sin(k_{xn}\xi),$$
$$Z_0 H_y(\xi, 0) = j \sum_n \left(\left(\frac{k_{xn}}{k} + \frac{k}{k_{xn}} \right) A_n + \frac{k_{xn}}{k} B_n \right) \times \sin(k_{xn}\xi). \tag{2}$$

The horizontal detuning impedance per unit length is then obtained from the EM fields at $(x, y) = (\xi, 0)$ for the source current I_0 at $(x, y) = (0, 0)$ given in Eq. (16) of Ref. [6]:

$$\begin{aligned} \frac{Z_h^{quad}}{L} &= \frac{j}{I_0 \xi} \left(E_x(\xi, 0) - Z_0 H_y(\xi, 0) \right) \\ &= \frac{1}{I_0 \xi} \sum_{n=0}^{\infty} \frac{k_{xn}}{k} (A_n + B_n) \sin(k_{xn}\xi) \\ &= -j \frac{Z_0}{2a\xi} \sum_{n=0}^{\infty} \frac{k_{xn}}{k} T_n \sin(k_{xn}\xi). \end{aligned} \tag{3}$$

with

$$T_n = \frac{1}{\frac{\frac{k_{xn}}{k}(1+\mu_r\varepsilon_r) sh\, ch + \frac{k_{yn}}{k}(\mu_r sh^2 tn - \varepsilon_r ch^2 ct)}{\mu_r\varepsilon_r - 1} - \frac{k}{k_{xn}} sh\, ch} \tag{4}$$

where we have $sh = \sinh(k_{xn}b)$, $ch = \cosh(k_{xn}b)$, $tn = \tan[k_{yn}(b-d)]$, $ct = \cot[k_{yn}(b-d)]$ and $k_{xn}^2 + k_{yn}^2 = k^2(\varepsilon_r\mu_r - 1)$. The boundary conditions (Eq. (19) in Ref. [6]) are valid and we have used the expression of $(A_n + B_n)$ given in Eq. (21) and (27) of Ref. [6]. We finally choose a small displacement ξ so that we can write to first order:

$$\frac{Z_h^{quad}}{L} = -j \frac{Z_0}{2a} \sum_{n=0}^{\infty} \frac{k_{xn}^2}{k} T_n. \tag{5}$$

It is interesting to note that the horizontal quadrupolar impedance at small transverse positions for each hybrid waveguide mode number is simply given by the longitudinal impedance multiplied by a factor $-\frac{k_{xn}^2}{k}$.

Vertical Quadrupolar Impedance

Similarly, the vertical detuning impedance can be obtained. At coordinate $(x, y) = (0, \xi)$, fields E_y and H_x in the vacuum region can be written

$$E_y(0, \xi) = \sum_n \frac{jk}{k_{xn}} B_n \sinh(k_{xn}\xi),$$
$$Z_0 H_x(0, \xi) = j \sum_n \left(\frac{k_{xn}}{k} A_n + \left(\frac{k_{xn}}{k} - \frac{k}{k_{xn}} \right) B_n \right) \times \sinh(k_{xn}\xi). \tag{6}$$

The vertical detuning impedance per unit length is obtained from the EM fields at $(x, y) = (0, \xi)$ for the source current I_0 at $(x, y) = (0, 0)$.

$$\begin{aligned} \frac{Z_v^{quad}}{L} &= \frac{j}{I_0 \xi} \left(E_y(0, \xi) + Z_0 H_x(0, \xi) \right) \\ &= -\frac{1}{I_0 \xi} \sum_{n=0}^{\infty} \frac{k_{xn}}{k} (A_n + B_n) \sinh(k_{xn}\xi) \\ &= j \frac{Z_0}{2a\xi} \sum_{n=0}^{\infty} \frac{k_{xn}}{k} T_n \sinh(k_{xn}\xi). \end{aligned} \tag{7}$$

We choose a small displacement ξ is so that we can write to first order:

$$\frac{Z_v^{quad}}{L} = j \frac{Z_0}{2a} \sum_{n=0}^{\infty} \frac{k_{xn}^2}{k} T_n. \tag{8}$$

In this case, we observe that $Z_v^{quad} = -Z_h^{quad}$, as was also expected by Tsutsui [12].

CASE OF AN SPS MKE KICKER

The dipolar and quadrupolar impedances in both planes are presented in Fig. 2 for a single SPS MKE kicker (MKE.61651). From this graph, we can conclude that impedance contributions can not be related by simple Yokoya factors. Also, looking specifically at the low frequency imaginary impedance, we observe that quadrupolar impedances are larger than dipolar impedances in each plane, inverting completely the picture obtained from the flat chamber model. The importance of the quadrupolar contribution is confirmed when summing all the kickers in the SPS. In fact, summing the dipolar and quadrupolar imaginary contributions in the horizontal plane yields a large negative horizontal impedance at low frequency, which could explain the positive tune shift observed in the SPS in the horizontal plane. The total dipolar and

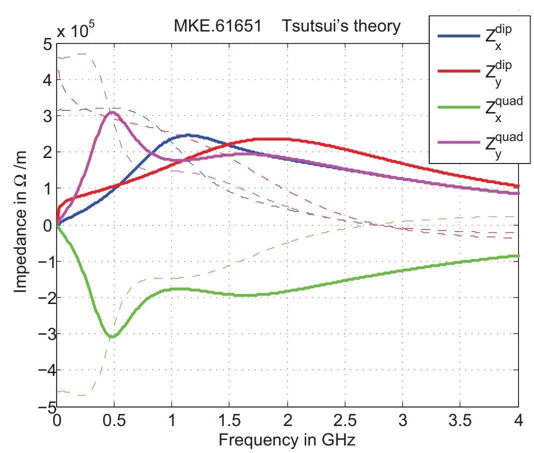

Figure 2: Dipolar and quadrupolar impedance in both transverse planes for SPS kicker MKE.61651. Real parts are full thick lines, imaginary parts are thin and dashed.

quadrupolar wake functions can be obtained through inverse Fourier Transform of the dipolar and quadrupolar impedance contributions. These wake functions are given in Fig. 3 together with the wake functions obtained with the flat chamber model in [13]. We see again the larger quadrupolar contributions in Tsutsui's model compared to Zotter/Métral's model, and we observe that their effect extends to trailing charges at larger distances from the source charge.

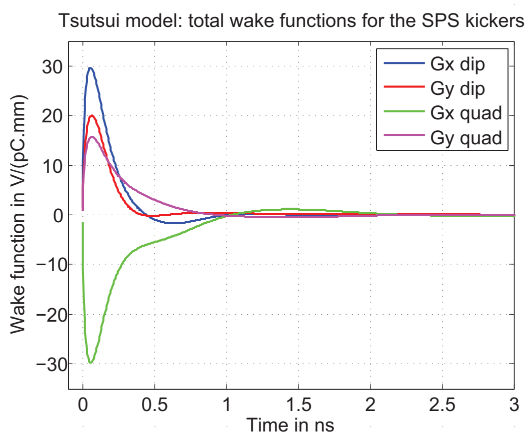

Figure 3: Total dipolar and quadrupolar wake functions in both transverse planes for all SPS kickers for Tsutsui's model.

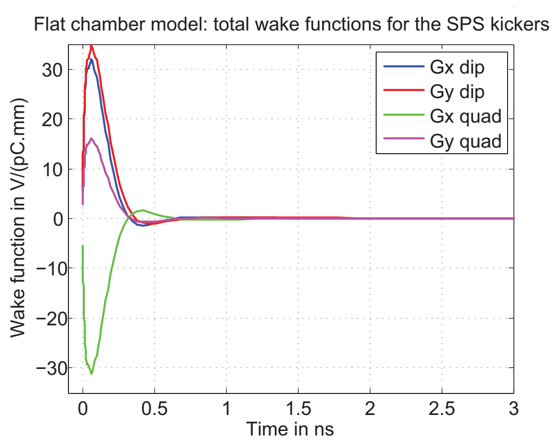

Figure 4: Total dipolar and quadrupolar wake functions in both transverse planes for all SPS kickers for the flat chamber model.

These analytical calculations have also been successfully benchmarked to CST Particle Studio 3D simulations of a simple model of kicker (right sketch in Fig. 1), and also to a more recent flat chamber theory in the limit for which the distance between the metal plates goes to infinity [15]. These simulations are described in detail in [14]. Finally, simulating the interaction of an SPS bunch with this new kickers model results in a positive horizontal tune shift, which lies within 10% of the tune shift measured with the SPS beam [13].

CONCLUSION

The formalism of Tsutsui was used to derive the quadrupolar impedance of a simple model of kicker. These formulae were successfully benchmarked to 3D EM simulations and could explain the positive tune shift measured with the SPS beam. However, the good agreement between the flat chamber model and bench measurements on an SPS MKE kicker proves us that Tsutsui's model is not yet a fully satisfying model for this case. As a consequence, the simple geometric model presented by Tsutsui and studied here is now being worked on so that 3D simulations can be performed with more realistic features (geometry, external circuits, metallic shielding, longitudinal cell structure, etc.).

REFERENCES

[1] E. Métral and B. Salvant, "Update on the SPS kickers", Presented at the CERN APC, 27 April 2007.

[2] E. Métral et al., "Resistive-Wall Impedance of an Infinitely long Multi-Layer Cylindrical Beam Pipe", Proc. PAC'07, Albuquerque, NM, USA, 2007.

[3] K. Yokoya, "Resistive Wall Impedance of Beam Pipes of General Cross Section", Part. Acc., 41, 221, 1993.

[4] E. Métral et al., "Kicker Impedance Measurements For The Future Multiturn Extraction Of The CERN Proton Synchrotron", Proc. EPAC'06, Edinburgh, Scotland, 2006.

[5] E. Métral, "SPS Impedance Budget Follow-up", Presented at the CERN SPS Impedance Meeting, 18 July 2008.

[6] H. Tsutsui, "Some Simplified Models of Ferrite Kicker Magnet for Calculation of Longitudinal Coupling Impedance", CERN-SL-2000-004 AP, 2000.

[7] H. Tsutsui, "Transverse Coupling Impedance of a Simplified Ferrite Kicker Magnet Model", LHC Project Note 234, 2000.

[8] F. Caspers et al, "Impedance Evaluation of the SPS MKE Kicker with Transition Pieces between Tank and Kicker Module", CERN-SL-2000-071 (AP), 2000.

[9] M.J. Barnes et al, "Measurement of the longitudinal and transverse impedance of kicker magnets using the coaxial wire method", Proc. PAC'09, Vancouver, BC, Canada, 2009.

[10] R.E. Collin, "Field Theory of Guided Waves", 2nd Edition, IEEE press, 1990.

[11] L. Xiao and W. Gai and X. Sun, "Field analysis of a dielectric-loaded rectangular waveguide in accelerating structure", Phys. Rev. E, 016505 (2001) 65.

[12] H. Tsutsui, "On single wire technique for transverse coupling impedance measurement", CERN SL-Note-2002-034 AP, 2002.

[13] B. Salvant, "Impedance model of the CERN SPS and aspects of LHC single-bunch stability", EPFL PhD Thesis 4585, 2010.

[14] C. Zannini et al, "Electromagnetic Simulations of Simple Models of Ferrite Loaded Kickers", these proceedings.

[15] N. Mounet and E. Métral, "Generalized Form Factors for the Beam Coupling Impedances in a Flat Chamber", these proceedings.